Topographic Evolution of Heat-Treated Nb Upon Electropolishing for SRF Applications

Work presented is based on our paper in Physical Review Accelerators and Beams:

https://doi.org/10.1103/PhysRevAccelBeams.26.103101

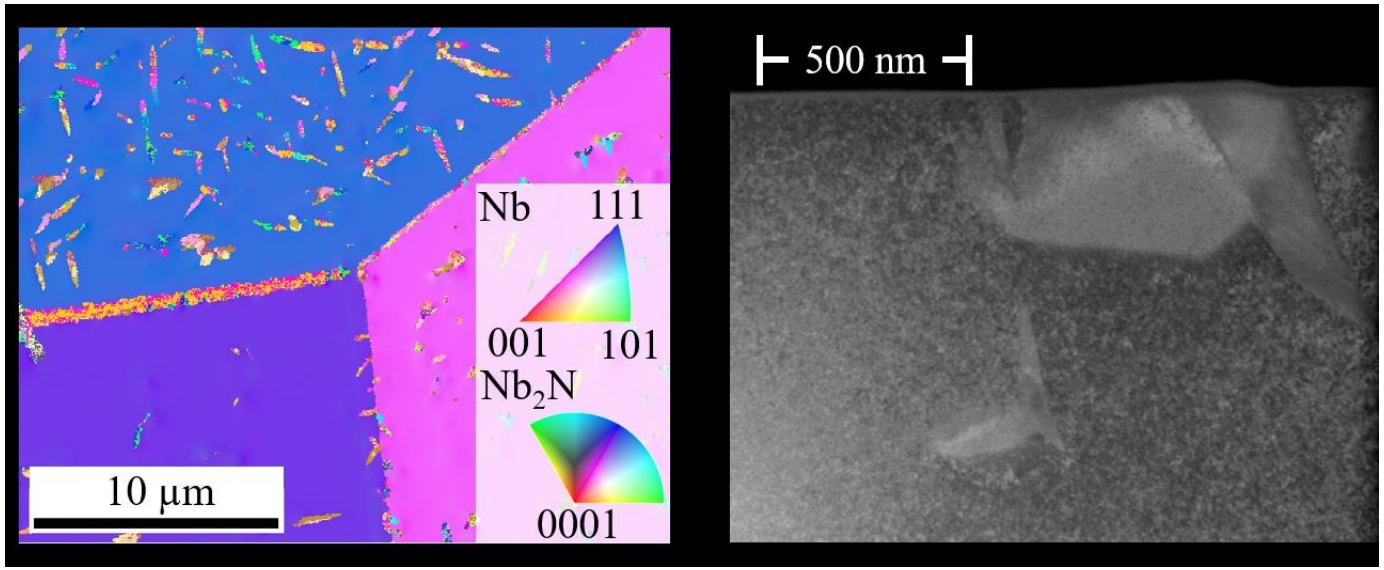

Eric M. Lechner

Jefferson Lab

U.S. DEPARTMENT OF ENERGY | Office of Science

JSA

Introduction – Importance of Impurities

[1]

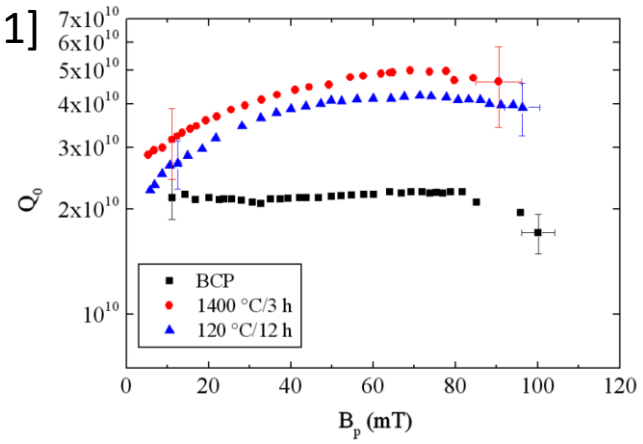

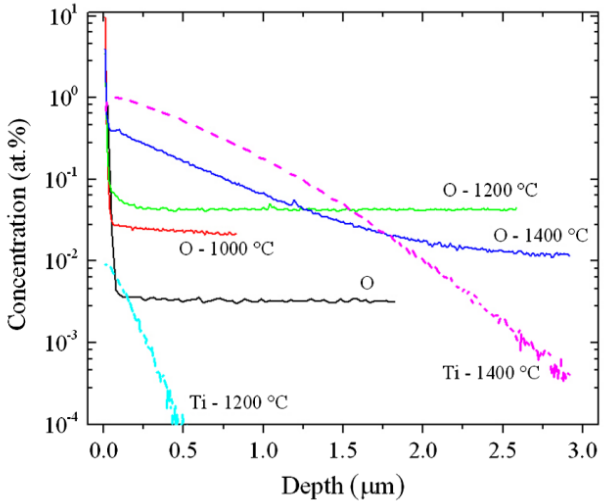

Ti impurities

[2]

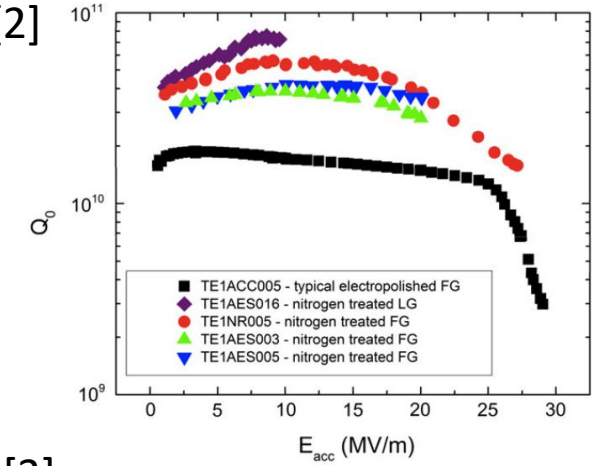

[3]

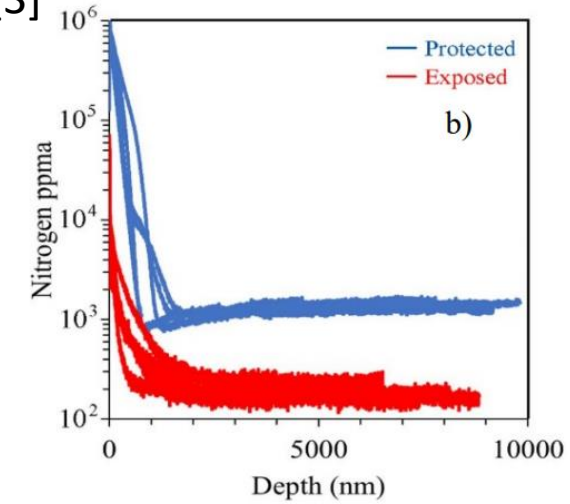

N impurities

[4]

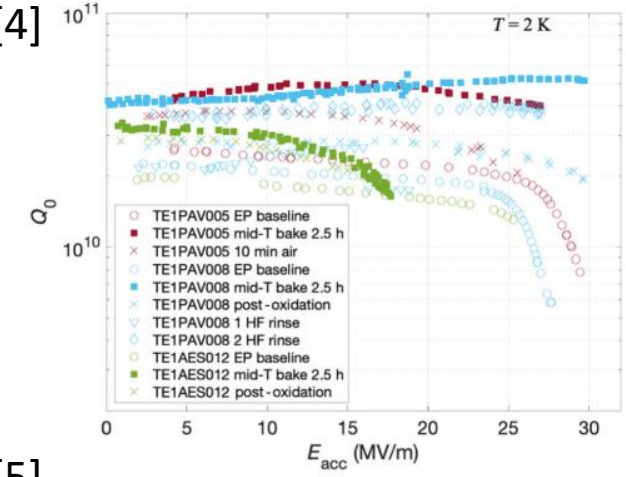

[5]

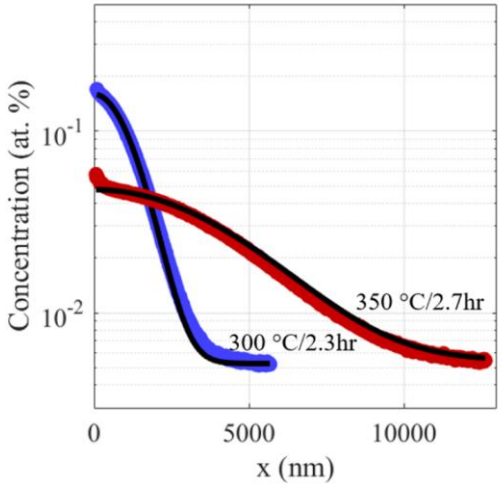

O impurities

- Introducing impurities has been an effective method for reducing the surface resistance at moderate accelerating gradients.
- N-doping successfully implemented in LCLS-II

[1] Dhakal, P., et al. *Physical Review Special Topics-Accelerators and Beams* 16.4 (2013): 042001.
[2] Grassellino, Anna, et al. *Superconductor Science and Technology* 26.10 (2013): 102001.
[3] Reece, Charles, et al. *Challenges to Reliable Production Nitrogen Doping of Nb for SRF Accelerating Cavities*. IPAC2022, 2022.
[4] Posen, S., et al. *Physical Review Applied* 13.1 (2020): 014024.
[5] Lechner, E. M., et al. *Applied Physics Letters* 119.8 (2021).

Jefferson Lab

Introduction – LCLS-II

[1] LCLS-II HE R&D

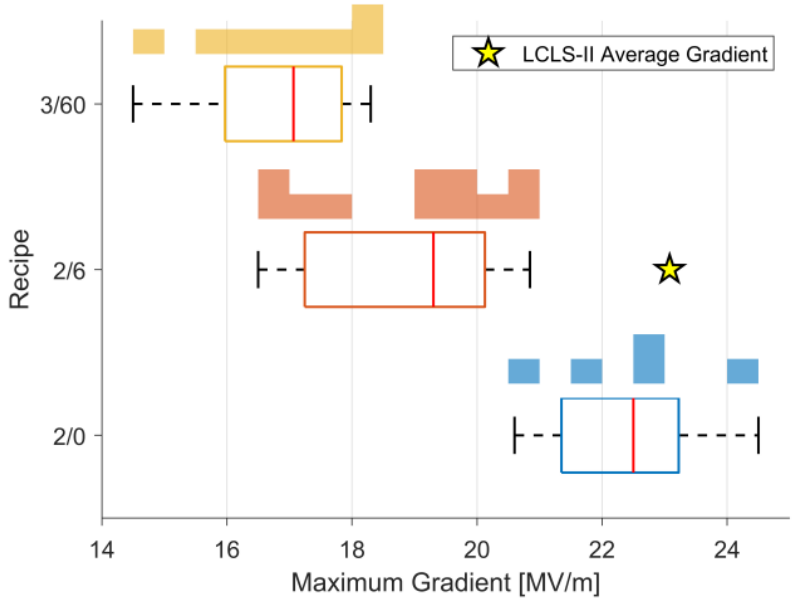

[2] LCLS-II Cavities (2N6)

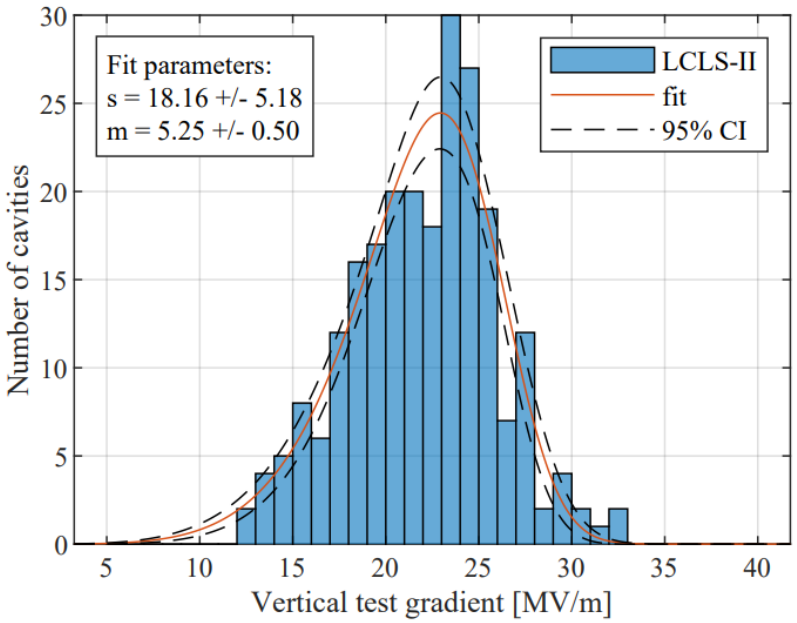

<E_{acc}> = 22 MV/m

[3] LCLS-II HE Cavities (2N0)

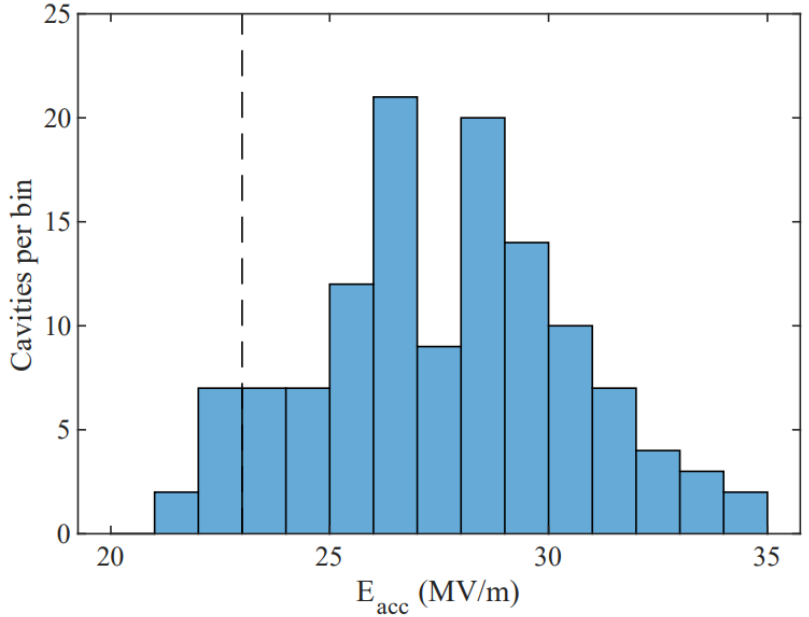

<E_{acc}> =27 MV/m

- Differences in max gradients observed in LCLS-II HE R&D
- What are the differences between the N doping heat treatments?

[1] Gonnella, Daniel, et al. *The LCLS-II HE high q and gradient r&d program*. SRF'19, 2019.
[2] Maniscalco, James, et al. *Statistical Modeling of Peak Accelerating Gradients in LCLS-II and LCLS-II-HE*. SRF'21, 2021.
[3] Maniscalco, James, et al. *LCLS-II-HE CAVITY QUALIFICATION TESTING.* SRF'23, 2023

Introduction – Topographic Defects

[1]

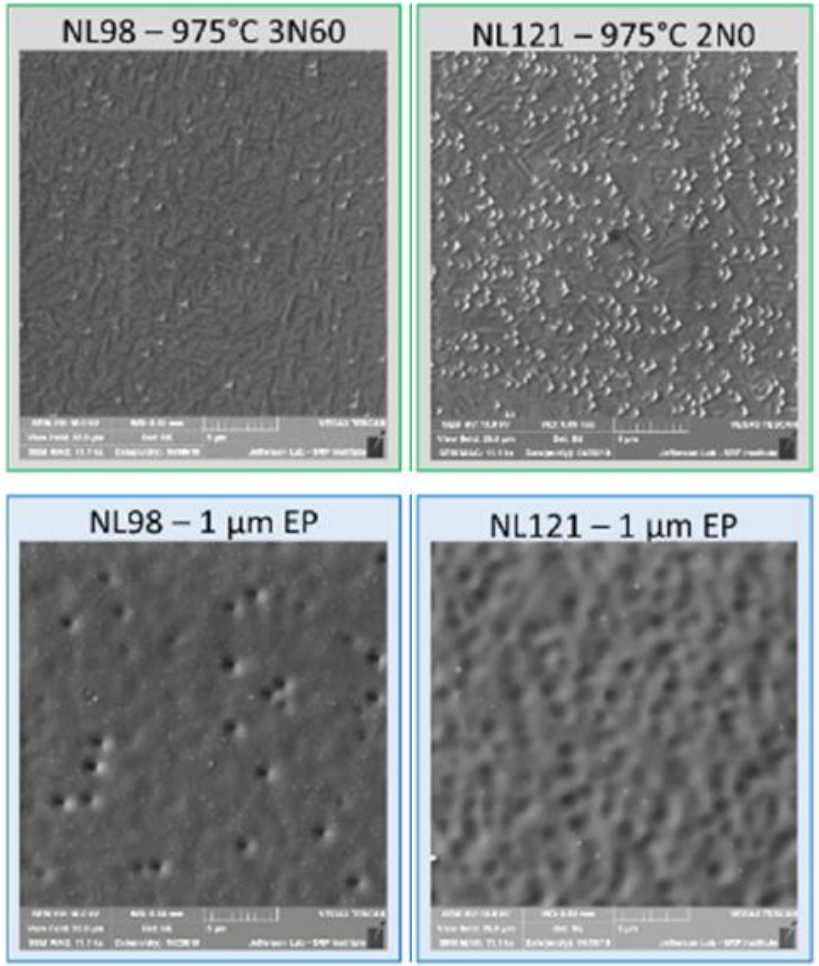

[2]

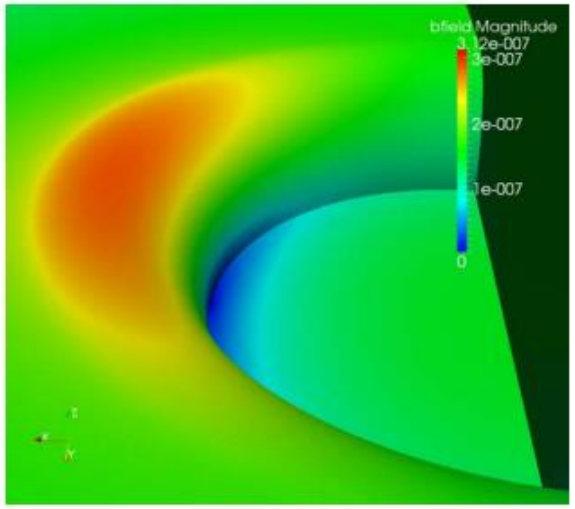

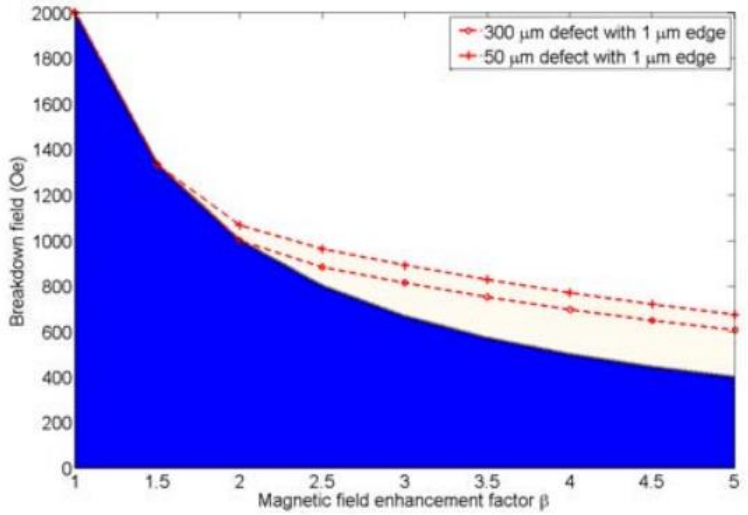

[3]

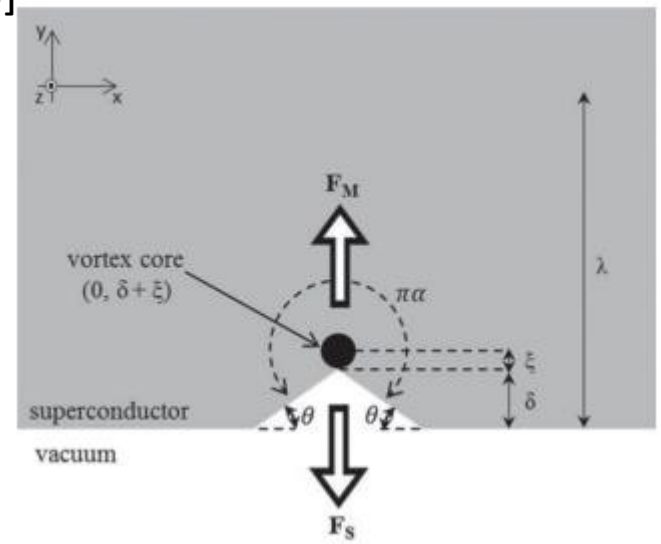

- In N doped Nb, EP reveals topographic defects within grains.
- Topographic defects produce local field enhancements due to the nature of the Meissner current. This may turn some regions of the cavity normal conducting and lead to thermal instabilities.
- Topographic defects can reduce the local superheating fields. This reduces the field required to nucleate dissipative vortex semiloops and may help trigger thermal instabilities.

[1] Spradlin, J.K., et al. *The LCLS-II HE high q and gradient r&d program*. SRF'19, 2019.
[2] Xie , et al. Quench Simulation Using a Ring-Type Defect Model SRF'11, 2011
[3] Kubo, Takayuki, *Progress of Theoretical and Experimental Physics* 2015.6 (2015): 063G01.

Jefferson Lab

Atomic Force Microscopy

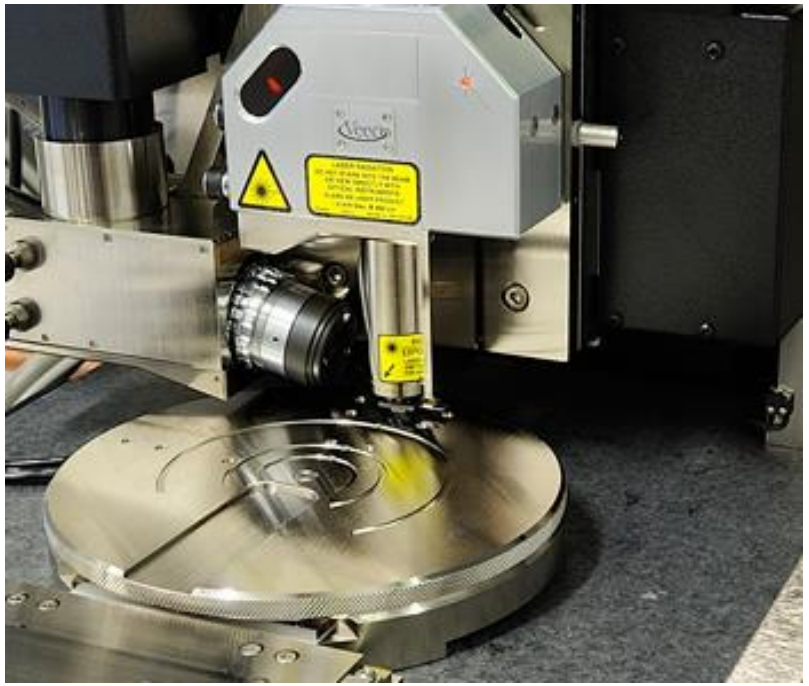

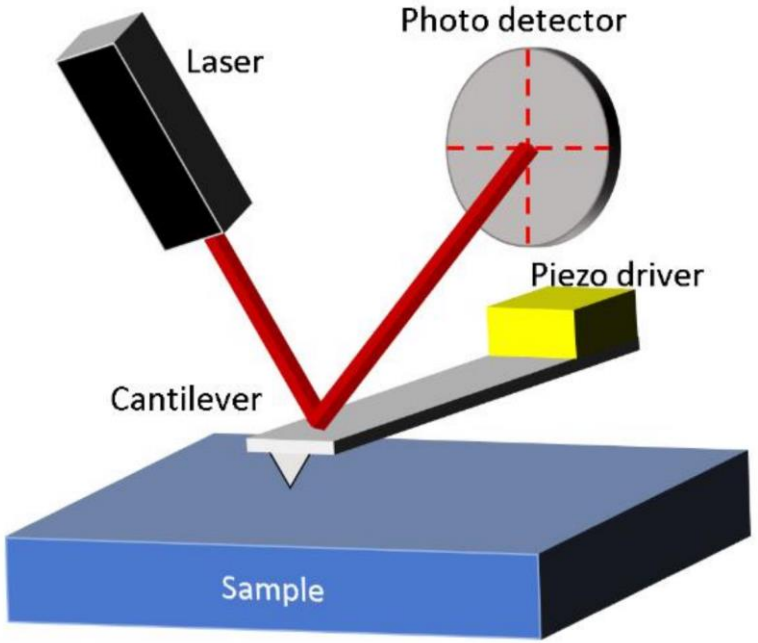

Pros

- < 10 nm tip radius allowing fantastic x-y spatial resolution on length scales relevant for SRF. Substantially better lateral resolution than WLI or LSCM

Cons

- Relatively slow.
- Limited to few-micron high and ~100 um wide scan areas.

Native Surface After Heat Treatment

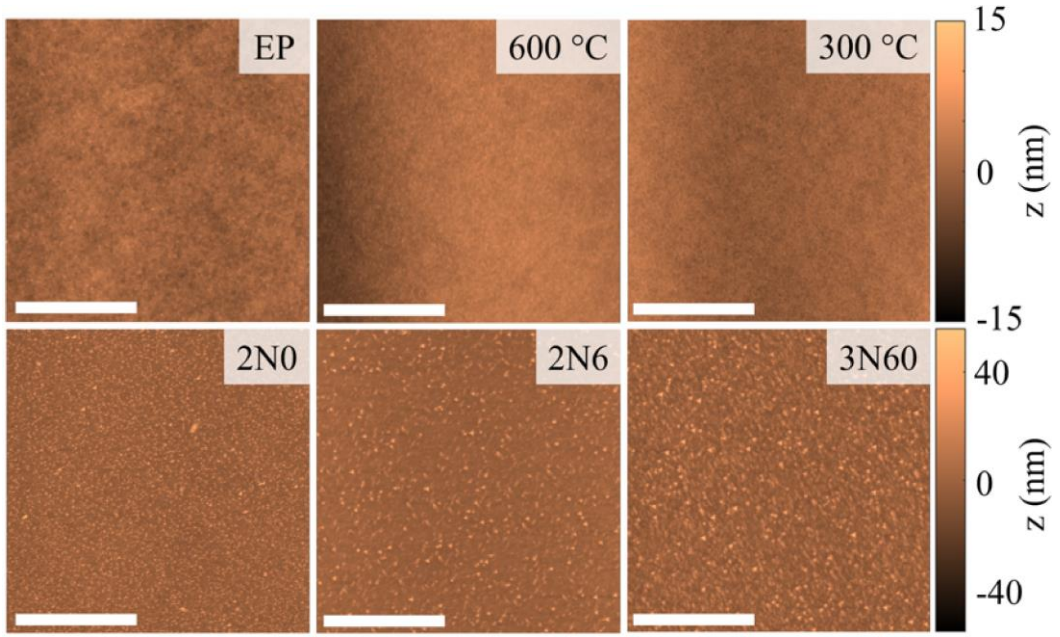

- Nitrides may form within, and continuously along some grain boundaries
- Niobium nitrides show sharp interfaces between surrounding doped Nb and nitride. Bad for magnetic field enhancement and superheating field suppression.

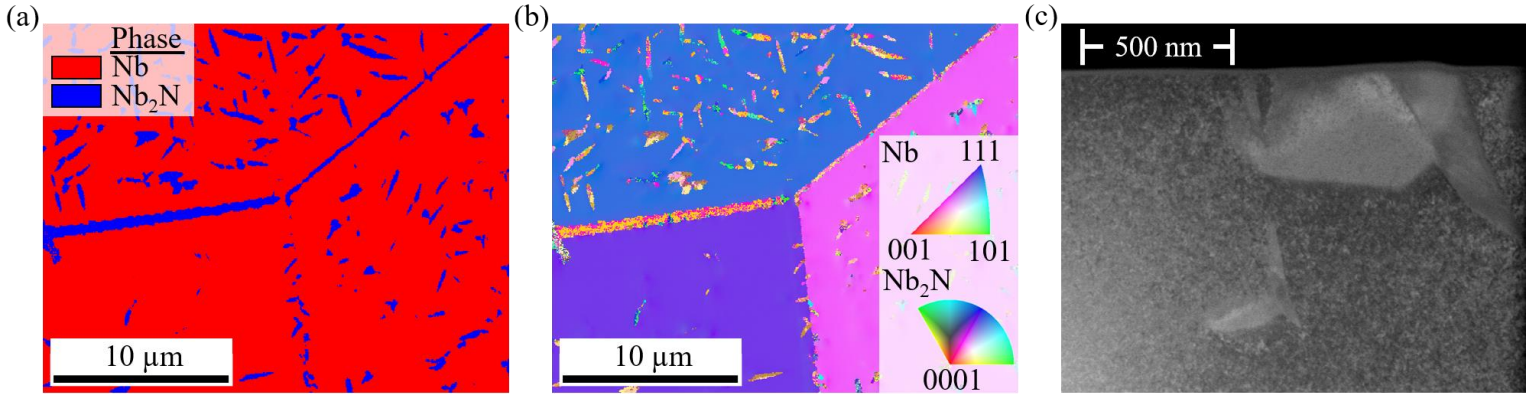

Jefferson Lab

Effect of EP on Heat-Treated Nb

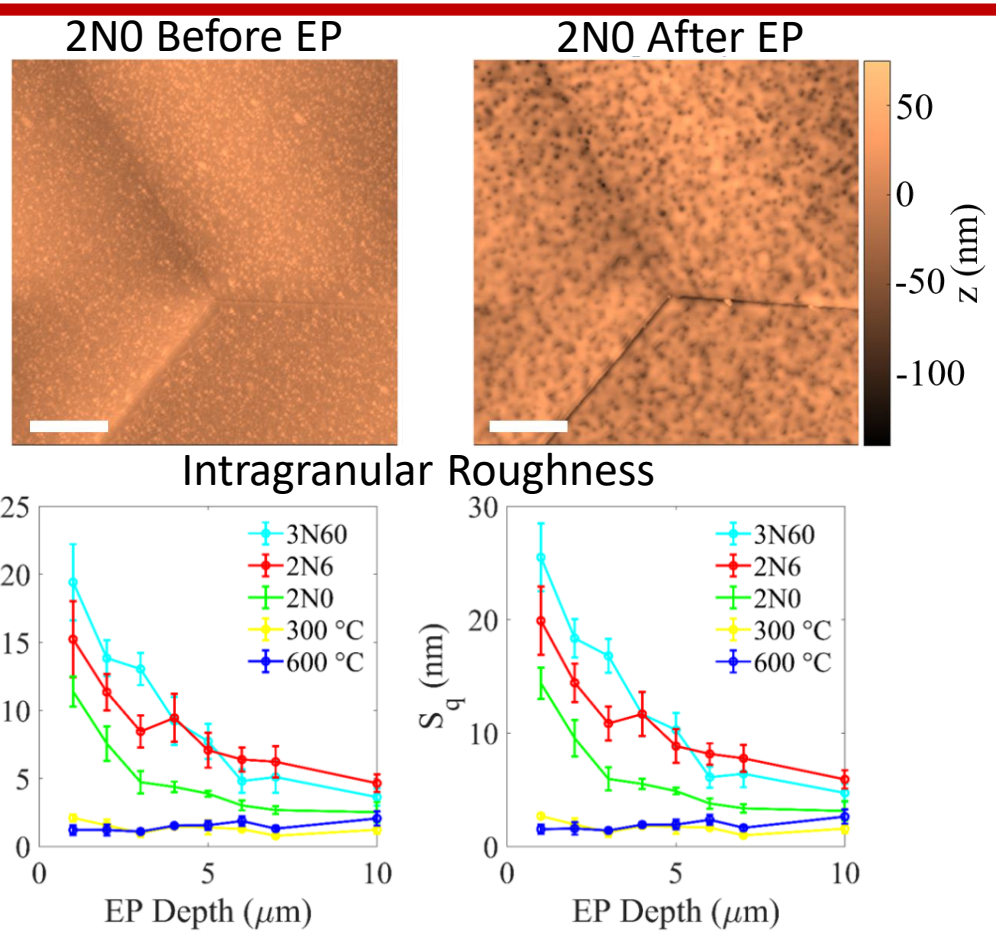

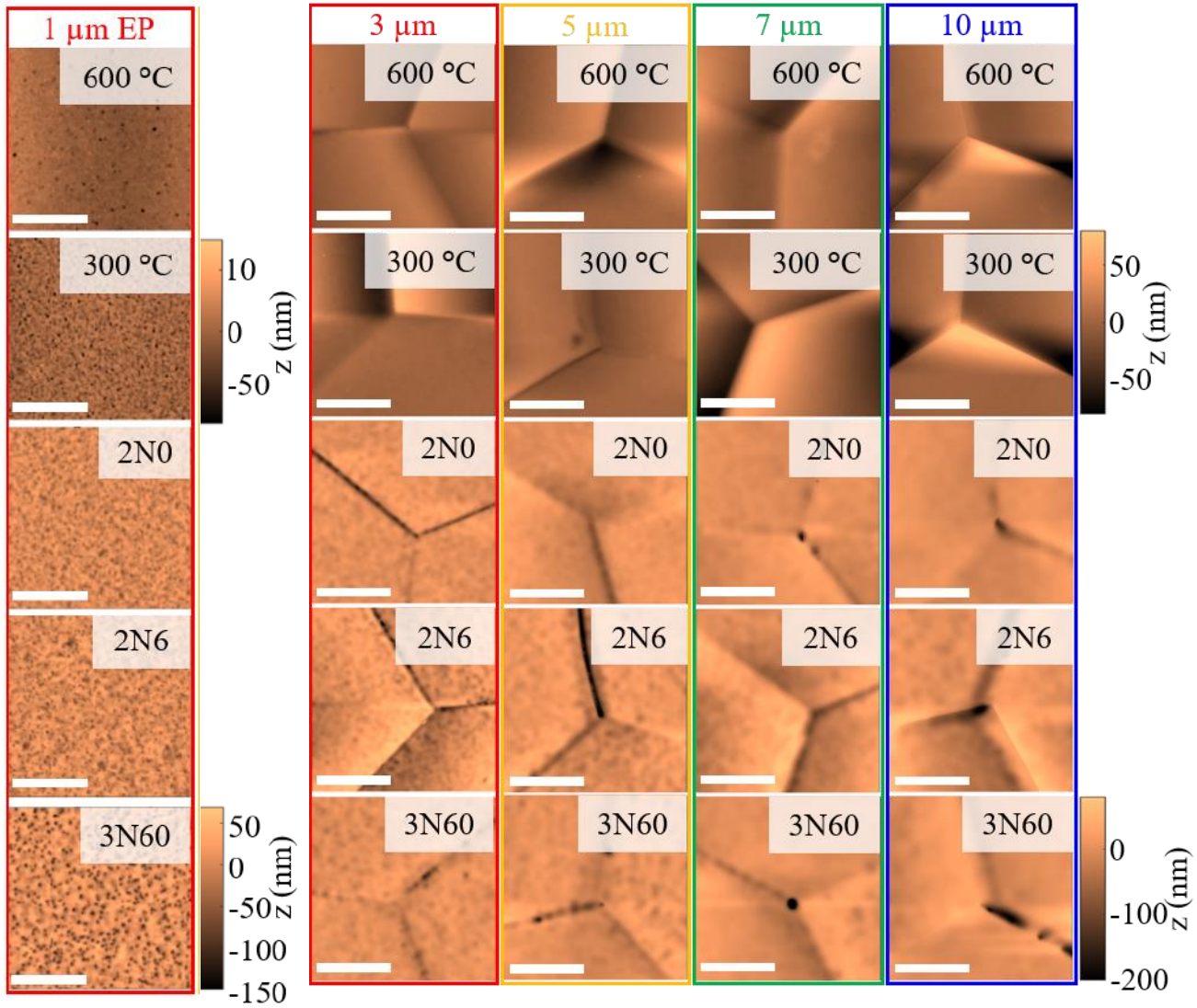

- When precipitates are present, electropolishing will attack the precipitate first which roughens the surface.
- Precipitates are worst in the N-doped samples especially at grain boundaries and triple junctions.
- Further EP smoothens the surface as expected.

Jefferson Lab

Topographic Magnetic Field Enhancement & Superheating Field Suppression

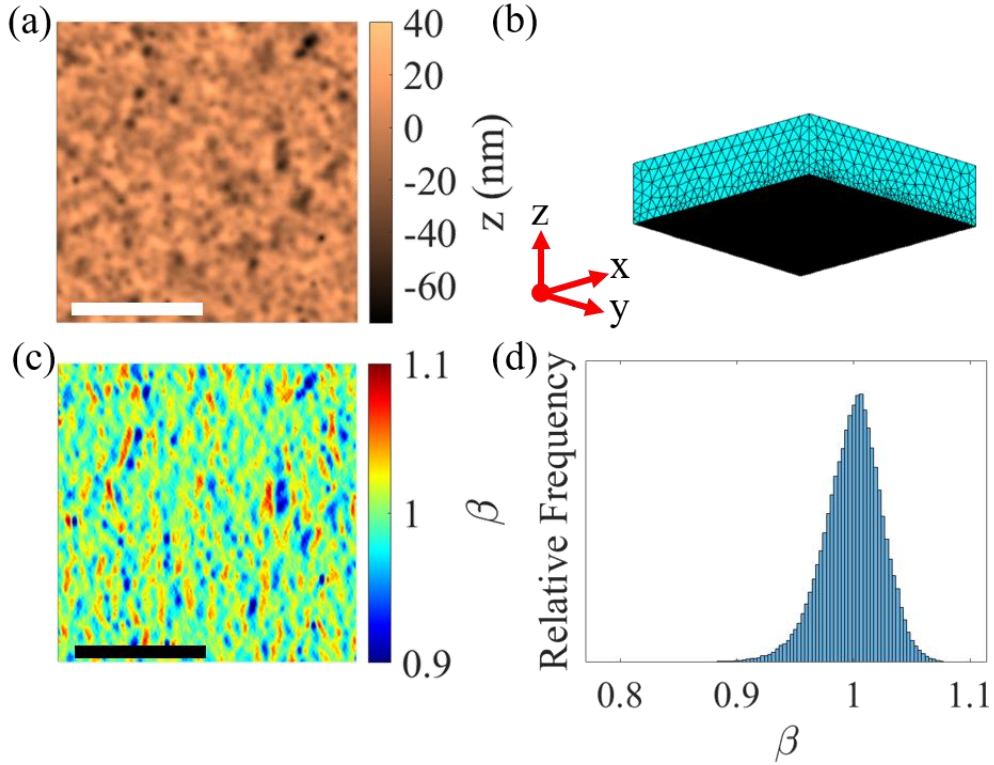

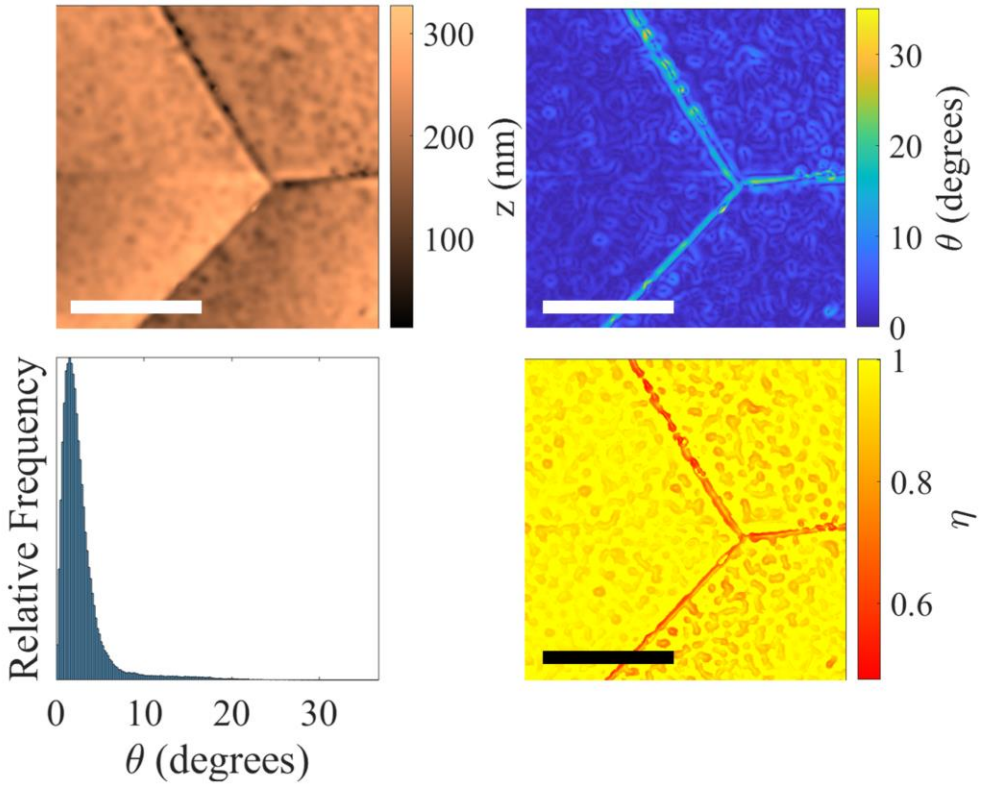

Magnetic Field Enhancement Factor

$$\beta(\mathbf{r}) = |\mathbf{B}(\mathbf{r})|/B_0$$

$$\nabla^2\psi = 0$$

$$\nabla\psi\cdot\hat{x} = B_0,\ \nabla\psi\cdot\hat{y} = 0 \text{ and } \nabla\psi\cdot\hat{n} = 0$$

$$\psi(x, y, z_{max} = 6\ \mu m) = -B_0 x\ \mathbf{B}(\mathbf{r}) = B_0\hat{x}$$

Superheating Field Suppression Factor

$$\tilde{B}_s = \eta B_s$$

$$\eta = \frac{1}{\alpha}\left(\frac{(\Gamma(\frac{\alpha}{2})\Gamma(\frac{3-\alpha}{2})\alpha\sin\left(\frac{\pi(\alpha-1)}{2}\right)}{\sqrt{\pi}}\frac{\xi}{\delta}\right)^{\frac{\alpha-1}{\alpha}}$$

$$\theta = \pi(\alpha-1)/2 \qquad \cos\theta = \hat{\mathbf{z}}\cdot\hat{\mathbf{n}} = \hat{\mathbf{z}}\cdot\frac{(-h_x, -h_y, 1)}{(1+h_x^2+h_y^2)^{\frac{1}{2}}}$$

Jefferson Lab

Topographic Superheating Field Suppression Factors

Superheating Field Suppression Factor Maps

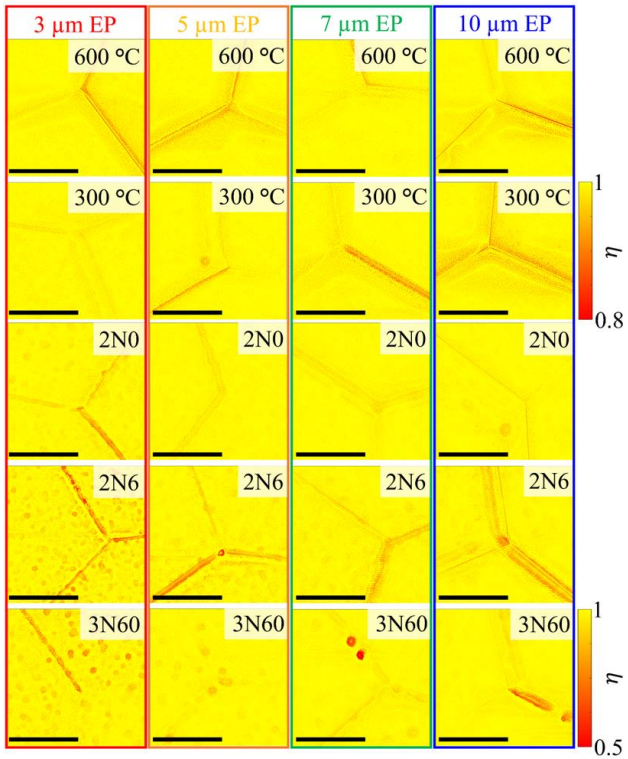

Intergranular Distribution

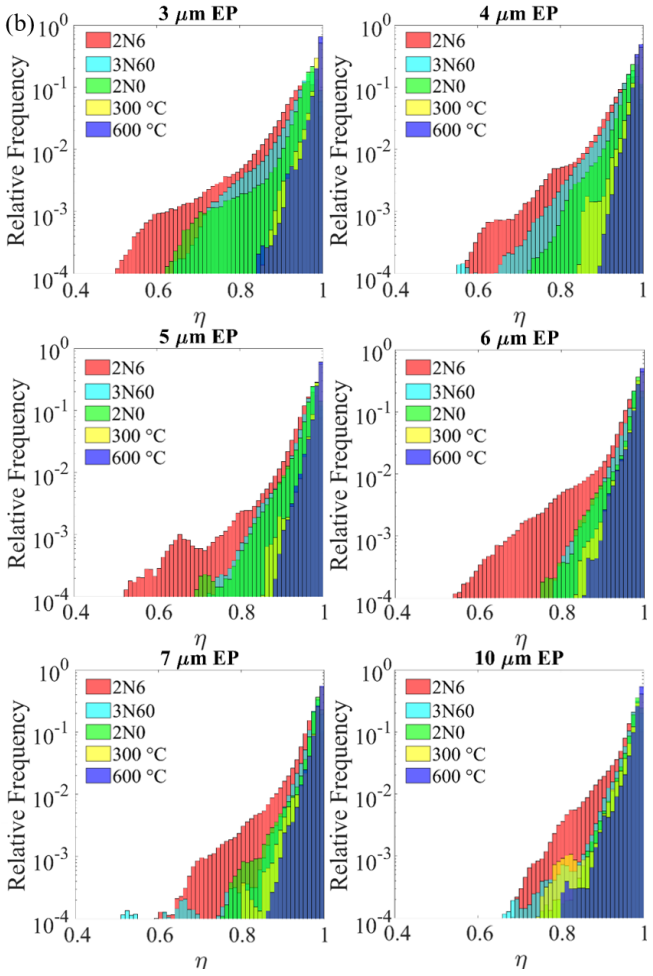

Intragranular Distribution

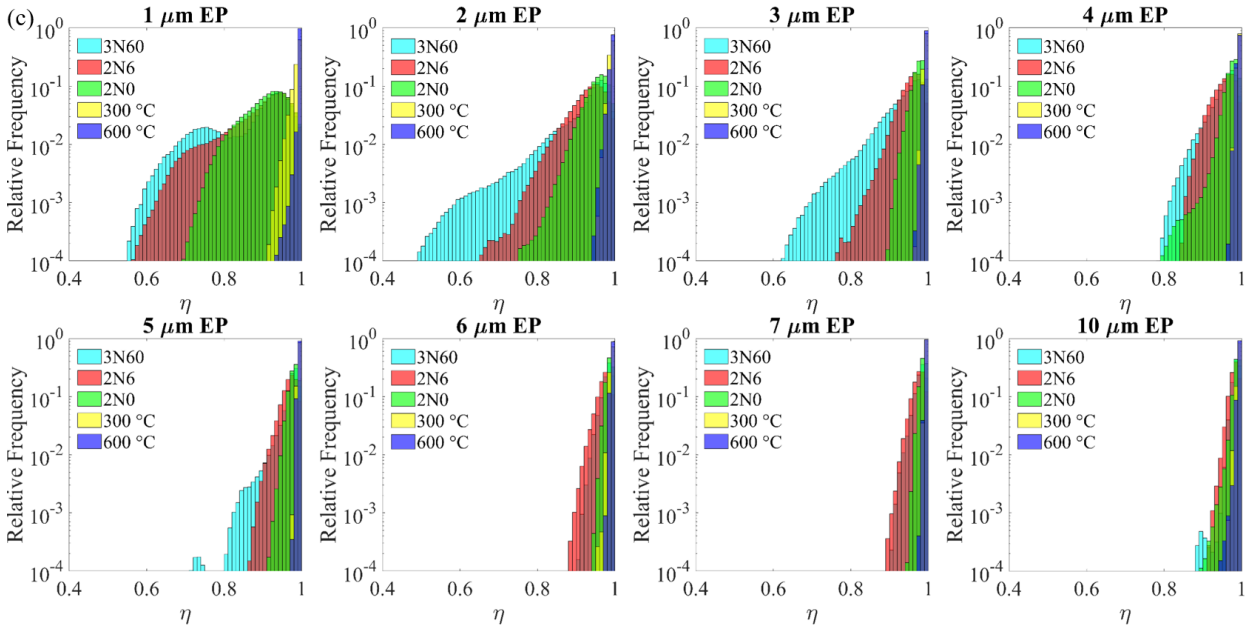

- Intragranular superheating field suppression is ameliorated first. With values of 0.9 at 7-10 μm EP
- The intergranular superheating field suppression factors are the most severe topographic defect which takes the longest to ameliorate with electropolishing. Even by 7-10 μm, values as low at 0.6-0.7 are observed.

Jefferson Lab

Topographic Magnetic Field Enhancement Factors

Magnetic Field Enhancement Factor Maps

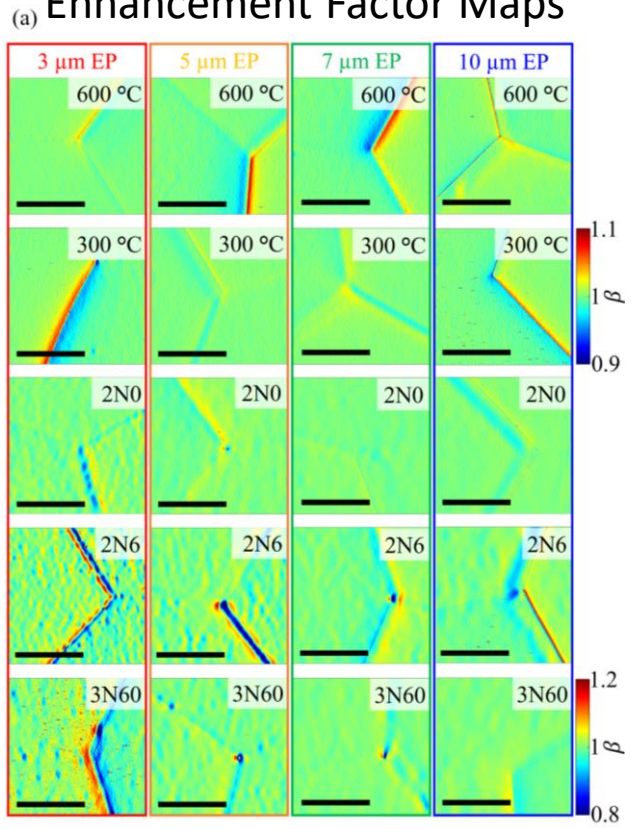

Intergranular Distribution

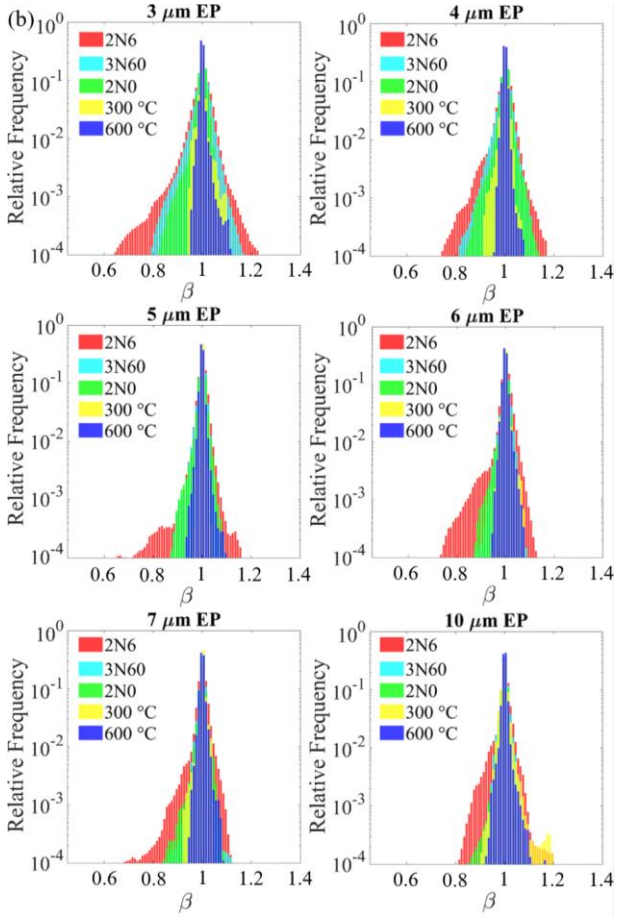

Intragranular Distribution

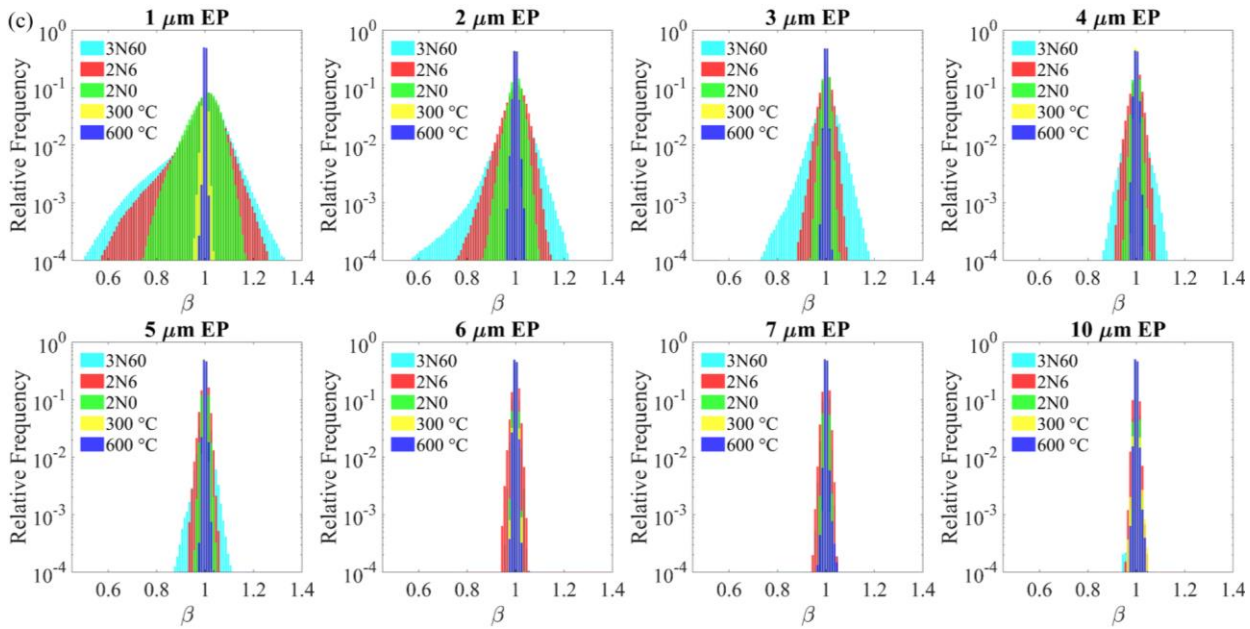

- Intragranular magnetic field enhancement factors are ameliorated first. With max values of 1.05 at 7-10 μm EP.
- The intergranular magnetic field enhancement factors are the found to be 1.1-1.2 between 7-10 μm, but this occurs for all samples examined. One would like to minimize intergranular steps from electropolishing.
- Between magnetic field enhancement and superheating field suppression, superheating field suppression values are substantially lower and may account for differences in performance for N-doped cavities.

Jefferson Lab

Effect of Impurities on the Superheating Field

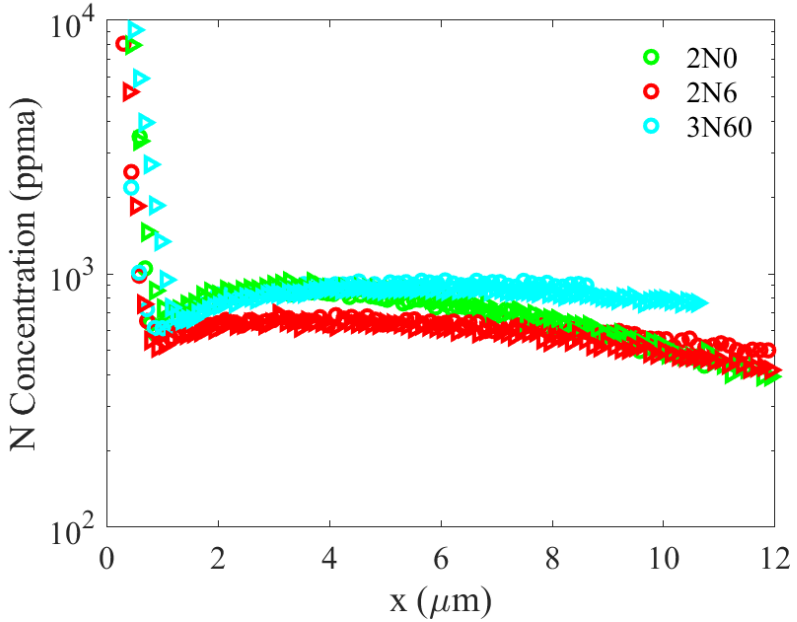

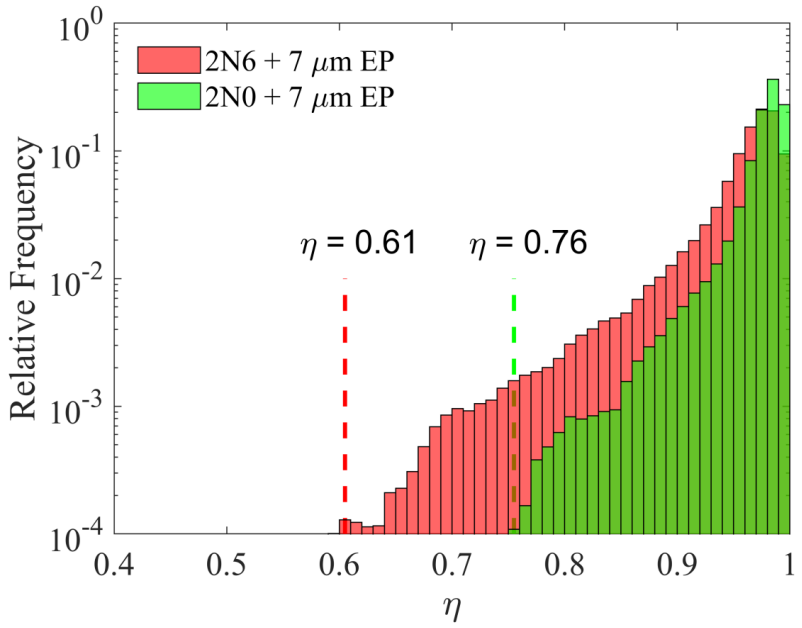

- The N impurity content in Nb between the different N doping surface treatments is small, at the target removal of 5-7 µm and 7µm for LCLS-II and LCLS-II HE the difference is negligible, pointing toward other sources of peak field degradation.
- The difference between superheating field suppression factors of 0.61 and 0.76 yield accelerating gradients of 23MV/m and 29MV/m before these loss mechanisms present themselves. This is in approximate agreement with the average quench fields observed in LCLS-II and LCLS-II HE.

[1]

$$\frac{H_{\mathrm{sh}}(\kappa)}{\sqrt{2}H_c} \approx \frac{\sqrt{10}}{6} + \frac{0.3852}{\sqrt{\kappa}}$$

- Negligible difference expected from change in κ

[1] Transtrum, Mark K., Gianluigi Catelani, and James P. Sethna. *Physical Review B* 83.9 (2011): 094505.

Conclusions & Future Work

Conclusions

- Highlighted severity of topographic defects within grains and along grain boundaries and investigated their topographic evolution with electropolishing.
- Small differences in N content between surface treatments indicates that perhaps differences impurity content plays a negligible role in peak field.
- Grain boundaries host the most severe topographic defects, both with magnetic field enhancement and superheating field suppression.
- Our topographic measurements may point to the mechanism behind the differences observed in the 2N0 and 2N6 processes for LCLS-II.
- In the vacuum heat treated samples, both magnetic field enhancement and superheating field suppression remain low which may allow the oxide dissolution process to achieve higher accelerating gradients (assuming carbides do not form).
- The topographic analysis methods presented here can be used to characterize the quality of various polishing methods and severity of topographic defects in materials beyond Nb.

Acknowledgments

Coauthors

C.E. Reece

M.J. Kelley

J.W. Angle (Now at PNNL)

C. Baxley

Others

G. Ciovati

O. Trofimova

R. Overton

T. Harris